Journal of Human Evolution 155 (2021) 102977

Contents lists available at ScienceDirect

Journal of Human Evolution

journal homepage: www.elsevier.com/locate/jhevol

Short Communications

Late Pleistocene partial femora from Maomaodong, southwestern China

Pianpian Wei [a], Zekun Weng [b, *], Kristian J. Carlson [c, d, *], Bo Cao [b], Li Jin [e, f], Wu Liu [g, h]

[a] Ministry of Education Key Laboratory of Contemporary Anthropology, Department of Anthropology and Human Genetics, School of Life Sciences, Fudan University, Shanghai, 200438, China
[b] Guizhou Municipal Institute of Cultural Relics and Archaeology, Guiyang, 5500044, China
[c] Department of Integrative Anatomical Sciences, Keck School of Medicine, University of Southern California, Los Angeles, CA 90033, USA
[d] Evolutionary Studies Institute, University of the Witwatersrand, WITS 2050, Johannesburg, South Africa
[e] State Key Laboratory of Genetic Engineering, Collaborative Innovation Center for Genetics and Development, School of Life Sciences, Fudan University, Shanghai, 200438, China
[f] Human Phoneme Institute, Fudan University, Shanghai, 200438, China
[g] Key Laboratory of Vertebrate Evolution and Human Origins, Institute of Vertebrate Palaeontology and Palaeoanthropology, Chinese Academy of Sciences, Beijing 100044, China
[h] CAS Center for Excellence in Life and Paleoenvironment, Beijing 100044, China

ARTICLE INFO

Article history:
Received 28 August 2020
Accepted 15 February 2021
Available online 23 April 2021

Keywords:
Femoral diaphysis
Robusticity
Cross-sectional geometry
Modern humans
East Asia

1. Introduction

Compared to the well-studied hominin postcranial skeleton from the Late Pleistocene to Early Holocene of Europe (Trinkaus, 2005, 2006, 2015; Trinkaus et al., 2014; Ruff et al., 2015; Villotte et al., 2020), studies on the hominin postcranial skeleton from the Late Pleistocene to Early Holocene of East Asia are rare, since the latter often lack secure chronological ages. The current hominin postcranial record from mainland East Asia associated with relatively accurate dates from this period includes fossils from Tianyuan Cave, Upper Cave, Maludong, and Zhaoguo cave. The Tianyuan 1 postcranial fossils (42–39 ka) are similar to those of early and recent modern humans with only few archaic features (Shang and Trinkaus, 2010; Wei et al., 2017). The original hominin femora from Upper Cave (35.1–10 ka; Chen, 1989, 1992; Li et al., 2018) were lost along with Zhoukoudian *Homo erectus* fossils during the Second World War, meaning only casts of their external surfaces are available for study (Wu, 1961). The Maludong site from southwestern China has yielded postcranial elements, including one femur (14.31 ± 0.34 to 13.59 ± 0.125 ka) that has been claimed to be more morphologically similar to those of archaic *Homo* than to those of modern humans, despite the relatively recent chronological age of the site (Curnoe et al., 2015). Finally, the postcranial elements recovered from Zhaoguo Cave (10.66–11.07 ka) in southwestern China indicate more modern human-like features compared with those of Maludong (Wei et al., 2020). Collectively, we are still far away from understanding the extent of regional postcranial morphological diversity during this period, and also the implications it may have for human evolution in mainland East Asia. Additional securely dated specimens are needed.

Here we describe and compare three partial femora from the site of Maomaodong in southwestern China dating to the Pleistocene–Holocene transition (14.5 ± 1.2 ka: Cao et al., 2015; Supplementary Online Material [SOM] Fig. S1). Details of the site are provided in SOM S1. These newly described and compared partial femora broaden morphological context for further understanding Late Pleistocene hominin morphological variation in the lower limbs and add to the current understanding of the origin and evolution of modern humans in East Asia and southwestern China in particular.

2. Materials and methods

2.1. Maomaodong femoral remains and comparative samples

The Maomaodong hominin partial femora are heavily mineralized and preserve different diaphyseal portions. Overlapping regions are preserved on GM7506 versus GM7507 or GM7508, while

* Corresponding authors.
E-mail addresses: 1513051739@qq.com (Z. Weng), kristian.carlson@usc.edu (K.J. Carlson).

https://doi.org/10.1016/j.jhevol.2021.102977
0047-2484/

clear size differences exist between the latter (GM7507 and GM7508; Fig. 1). This suggests the likely presence of three individuals comprising the sample. To broadly place Maomaodong femora within temporal variation exhibited by Pleistocene hominin femora, five comparative groups (SOM Table S1) were compiled from published studies (Puymerail et al., 2012; Trinkaus and Ruff, 2012; Chevalier et al., 2015; Ruff et al., 2015; Rodríguez et al., 2018): Early Pleistocene (EP; >780 ka), early Middle Pleistocene (EMP; 400–780 ka), late Middle Pleistocene (LMP; 126–400 ka), Neandertals (Nea.), and Late Pleistocene modern humans (LPMH; 11.7–126 ka). Additionally, one Holocene modern human sample from China (MH) was selected for comparisons: the Datong population (n = 24) from Beiwei Dynasty during the 5th century in Datong City, Shanxi province, northern China (Han, 2005; Wei et al., 2017; Xing et al., 2018).

2.2. Microcomputed tomography and acquisition of cross sections

Maomaodong femora were scanned using the 450 kV industrial μCT system developed by the Institute of High Energy Physics, Chinese Academy of Sciences (CAS) at the Key Laboratory of Vertebrate Evolution and Human Origins. Details on scanning parameters, femoral positioning, and estimation of locations of 50% and 80% diaphyseal cross sections are provided in SOM S2. Following the orientation protocol (Ruff, 2002; Carlson, 2005), anatomical criteria preserved on external surfaces were used to corroborate estimated diaphyseal locations after which cross sections were extracted for analyses (SOM S2; SOM Fig. S2).

2.3. Cross-sectional properties and femoral midshaft osteometric measurements

Cross-sectional geometric (CSG) properties, including subperiosteal area (TA), cortical area (CA), second moments of area (I_i), polar moment of area (J), and section moduli (Z_i), were calculated on cross-sectional images using the MomentMacroJ_v1_4B plugin (available at https://www.hopkinsmedicine.org/fae/mmacro.html) for ImageJ2 software (NIH, Bethesda, MD, USA; Abràmoff et al., 2004). To evaluate the relative distribution of bone within sections and/or relative rigidities of femoral cross sections in different orientations, we calculated ratios between properties, i.e., percent cortical area (% CA = CA/TA*100), anteroposterior vs. mediolateral second moments of area (I_x/I_y ratios), and maximum vs. minimum second moments of area (I_{max}/I_{min} ratios, as cross-sectional shape indices; e.g. Trinkaus and Ruff, 1989) using SPSS v. 20.0 (IBM Corp., 2017).

To account for potential error during orientation of partial specimens without preserved articular ends (i.e., identification of anteroposterior and mediolateral anatomical axes in cross sections), we estimated some properties about these axes by calculating them for cross sections that were rotated in 5° increments in either direction from our initial estimation. This provided a conservative range of values for cross-sectional properties calculated with respect to anteroposterior and mediolateral anatomical axes.

Since Cao et al. (2015) reported external diameters without providing details on bone orientation or without citing a measurement definition, we remeasured anteroposterior and mediolateral diameters at estimated midshaft and subtrochanteric locations of the Maomaodong femora. These osteometric measurements are quantified following definitions of Martin (Bräuer, 1988). We also report midshaft cross-sectional shape of the femoral diaphyses using ratios of the two external diameters (pilastric index: M-6/M-7).

3. Results

3.1. Descriptive morphology

3.1.1. GM7506 The right femur GM7506 consists of a partial diaphysis preserving approximately the mid-proximal to mid-distal region. Maximum length of the shaft fragment is 157.4 mm. Due to incomplete preservation, anteroposterior (AP) diaphyseal curvature cannot be quantified. Qualitatively, however, it is clear that a small amount of AP curvature exists. The proximal diaphyseal break is relatively clean and occurs in a transverse plane located distal to the spiral, pectineal, and gluteal lines, removing some of the inferior parts of all three. The proximal break also reveals a thick cortical wall, with the anterior region being relatively thinner than other regions. Medially, there is a narrow bulge in the diaphysis extending from the medial edge of the linea aspera and running anterosuperiorly until interruption by the proximal break (GM7506 posterior and medial view in Fig. 1). Posteriorly, the linea aspera is prominent on the surface and accompanies a pilaster, clearly aligned in form with those of femora of early modern humans (Trinkaus, 2005, 2006). Muscle attachments on the linea aspera are rugose and present as parallel medial and lateral ridges at the proximal break, suggesting that it occurs in the area of the mid-proximal

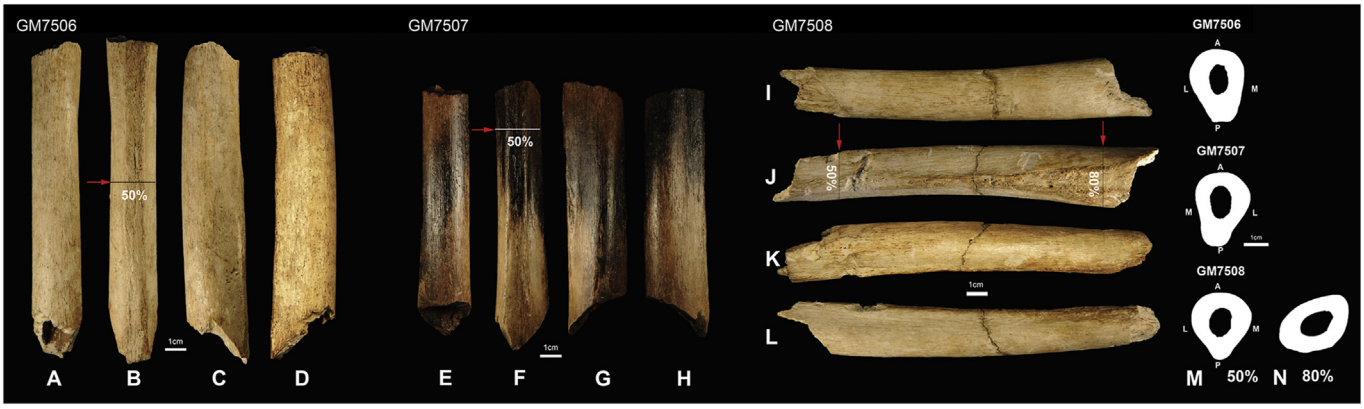

Figure 1. Maomaodong femora: A–D) right femur GM7506, in anterior (A), posterior (B), medial (C) and lateral (D) views; E–H) left femur GM7507, in anterior (E), posterior (F), medial (G) and lateral (H) views; I–L) right femur GM7508, in anterior (I), posterior (J), medial (K) and lateral (L) views. Estimated locations of cross sections for midshaft (50%; M) and subtrochanteric regions (80%; N) are indicated on diaphyses by red arrows. Abbreviations: A = anterior; P = posterior; M = medial; L = lateral cortices. (For interpretation of the references to color in this figure legend, the reader is referred to the Web version of this article.)

Table 1
Cross-sectional geometric parameters and osteometrics of Maomaodong femoral diaphyses.

Measurement	GM7506	GM7507	GM7508
50%			
TA (mm^2)	525	488	483
CA (mm^2)	449	402	401
I_x[a] (mm^4)	30,199 (29,661–30421)	26,715 (26,225–27041)	20,469 (20,422–20478)
I_y[a] (mm^4)	15,907 (15,578–16370)	13,601 (13,295–14131)	16,570 (16,566–16609)
I_{max} (mm^4)	30,548	27,148	20,473
I_{min} (mm^4)	15,558	13,167	16,566
J (mm^4)	46,106	40,315	37,039
Z_x[a] (mm^3)	1905 (1861–1906)	1690 (1672–1697)	1350 (1346–1354)
Z_y[a] (mm^3)	1332 (1332–1337)	1160 (1160–1169)	1324 (1300–1350)
Z_p (mm^3)	2842	2496	2444
M[b]-7 (mm)	23	22	25
M[b]-6 (mm)	30	30	27
80%			
TA (mm^2)	—	—	513
CA (mm^2)	—	—	416
I_x[a] (mm^4)	—	—	17,501 (16,298–18808)
I_y[a] (mm^4)	—	—	26,567 (25,217–27689)
I_{max} (mm^4)	—	—	30,492
I_{min} (mm^4)	—	—	13,576
J (mm^4)	—	—	44,068
Z_x[a] (mm^3)	—	—	1427 (1407–1443)
Z_y[a] (mm^3)	—	—	1807 (1760–1837)
Z_p (mm^3)	—	—	2685
M[b]-9 (mm)	—	—	31
M[b]-10 (mm)	—	—	20

Abbreviations: TA = total area; CA = cortical area; I_x = anteroposterior second moment of area; I_y = mediolateral second moment of area; I_{max} = maximum second moment of area, I_{min} = minimum second moment of area; J = polar moment of area; Z_x = anteroposterior section modulus; Z_y = mediolateral section modulus; Z_p = polar section modulus; M-7 = midshaft mediolateral diameter; M-6 = midshaft anteroposterior diameter; M-9 = proximal mediolateral diameter; M-10 = proximal anteroposterior diameter.

[a] Although we align Maomaodong femora to the same, single complete femur of a recent modern human (SOM S2; SOM Fig. S2), there is variation in their linea aspera morphology. Considering that there may be slight angle errors in the estimated orientations of the Maomaodong femora because of the absence of their articular ends, we report a range of second moments of area and section moduli calculated about their anteroposterior and mediolateral anatomical axes. This range reflects 5° clockwise and counterclockwise rotations (values in parentheses) with the estimated original orientation described as 0°.

[b] M refers to the measurement as defined in the Martin system (Bräuer, 1988).

diaphysis. Distally, the linea aspera has begun diverging into medial and lateral supracondylar lines immediately before interruption by the distal break. Thickness of the cortical wall at the distal break is uniformly thinner than thickness at the proximal break, while the diaphyseal cross section at the distal end is more anteroposterior elongated (GM7506 in Fig. 1).

3.1.2. GM7507 The left femur GM7507 consists of a partial diaphysis preserving middle to mid-distal regions (Fig. 1). Maximum length of the shaft fragment is 122.3 mm. The surface of the entire proximal half of the preserved diaphysis, along with the anterior surface of the remaining distal half, is darkly stained. Other surfaces do not appear stained, nor do either of the other partial femora (GM7506 and GM7508). Staining throughout the cortical thicknesses exposed at the proximal and distal breaks suggests that either the dark staining infiltrated the entire cortical thickness of the partial femur, or else the staining occurred after the femur was broken. Due to incomplete preservation, anteroposterior curvature of the diaphysis cannot be quantified. The cross section at the proximal break is markedly anteroposterior elongated. Compared to the right partial femur (GM7506), the presence of a bulge in the medial aspect of the diaphysis of GM7507 cannot be assessed because its proximal break occurs inferior to the comparable location of the bulge on GM7506. Posteriorly, the linea aspera is prominent, especially in the proximal half of the fragment, and accompanies an obvious pilaster that is typical on early modern human femora (Trinkaus, 2005, 2006). Muscle attachment sites along the linea aspera are rugose. The distal break occurs below where the linea aspera has clearly begun diverging into medial and lateral supracondylar lines. Thickness of the cortical wall at the distal break is uniformly thinner than thickness at the proximal break, while the diaphyseal cross section at the distal end is slightly anteroposteriorly elongated.

3.1.3. GM7508 The right femur (GM7508) is a partial diaphysis preserving from the distal border of the lesser trochanter until the midshaft region (Fig. 1). Maximum length of the shaft fragment is 186.2 mm. Qualitatively, anteroposterior curvature of the diaphysis is present, but it is not quantified due to the incomplete state of preservation. The proximal diaphyseal break is clean, with the medial region extending more proximally than other regions. It reveals a uniformly thin cortical wall, with a marked mediolaterally elongated cross section. There is a small area of bone missing from the anterior surface at the proximal break. Muscle attachment sites on the posterior surface of the proximal end are rugose. Posteriorly, the spiral line, pectineal line, and gluteal tuberosity are present, suggesting that the proximal break occurs proximal to the mid-proximal diaphysis (i.e., the specimen retains an 80% length or subtrochanteric cross section). There is an oblique break through the mid-proximal diaphysis, with a small area of bone loss on the anterior surface; the two portions rejoin cleanly. The linea aspera is relatively prominent, especially on the distal portion of the partial femur, with a relatively less developed pilaster than appears on GM7506 and GM7507. Muscle attachment sites along the linea aspera are also less rugose than those of GM7506 and GM7507. A nutrient foramen opens distally on the linea aspera about 2–3 cm below the proximal break. The anteroposterior shaft dimension narrows before interruption by the distal break. Thickness of the cortical wall at the distal break is uniformly thicker than thickness of the cortical wall at the proximal break, except in the lateral regions of the respective cross sections. The diaphyseal cross section at the distal break is more anteroposteriorly elongated than the diaphyseal cross section at the proximal break. Maximum mediolateral diameter of the partial femur, which occurs at its proximal break, is 31.2 mm, taken at the maximum development of the gluteal buttress (M-9; Bräuer, 1988).

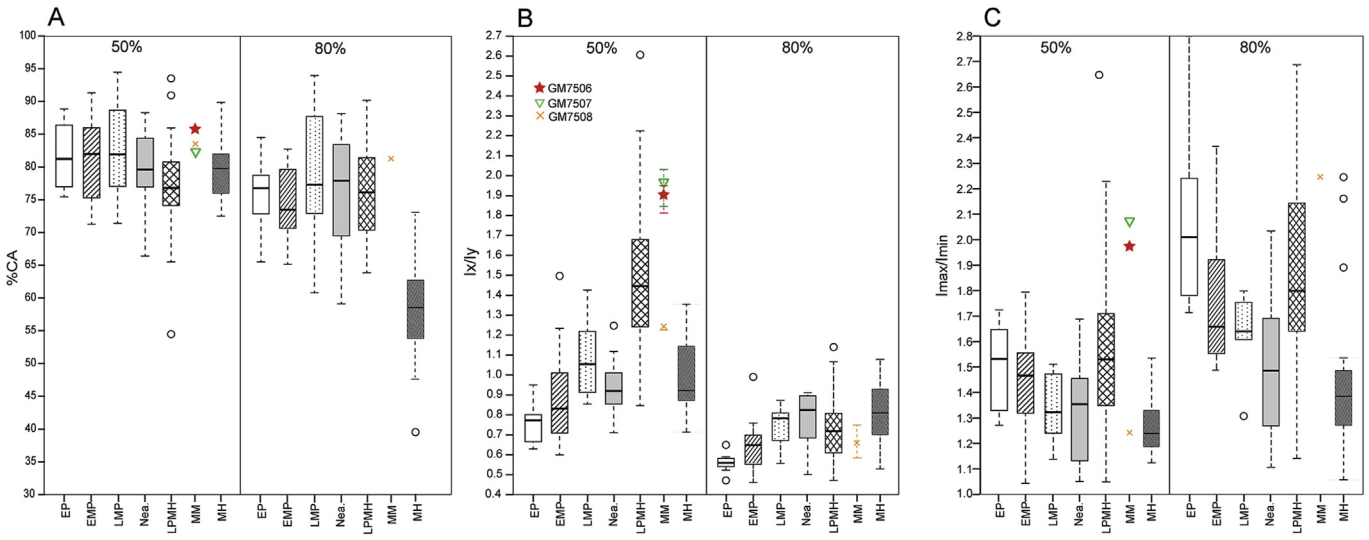

Figure 2. Comparative values of %CA (A), I_x/I_y (B), and I_{max}/I_{min} (C) measured at estimates of 50% and 80% biomechanical length in Maomaodong femora (GM7506, 7507, and 7508) and five Pleistocene hominin groups. Within box plots of comparative samples, the median (horizontal bar), upper and lower quartiles (boxes), and the upper and lower non-outlier extremes (vertical bar) are illustrated. For Maomaodong femora, original properties (i.e., cross sections with 0° rotations; colored geometric shapes) and adjusted properties (i.e., cross sections with 5° rotations; vertical bars) are illustrated. Note that each Maomaodong femur does not preserve both estimated locations due to differences in their preservation. Abbreviations: MM = Maomaodong; EP = Early Pleistocene; EMP = Early Middle Pleistocene; LMP = Late Middle Pleistocene; Nea = Neandertals; LPMH = Late Pleistocene Modern Humans; MH = Recent modern human sample. Fossils comprising groups are reported in SOM Table S1.

The corresponding anteroposterior diameter of the preserved diaphysis is 19.9 mm at the proximal break, taken at the maximum development of the gluteal buttress (M-10; Bräuer, 1988).

3.2. Comparative morphology

CSG parameters are provided in Table 1 and illustrated in Figure 2. In the estimated midshaft region, there are significant differences in %CAs among all comparative groups (see SOM Table S1; H = 14.716, df = 6, $p = 0.023$). Notably, the LPMH group is significantly lower in %CA at this cross section than the EP ($p = 0.026$), EMP ($p = 0.027$), and LMP ($p = 0.025$) groups. There are also significant group differences in the subtrochanteric region (80%; H = 51.684, df = 6, $p < 0.001$). Notably, the MH group is significantly lower in %CA than the EP ($p = 0.004$), EMP ($p = 0.002$), LMP ($p < 0.001$), Nea. ($p < 0.001$), and LPMH ($p < 0.001$) groups. The Maomaodong femora fall in the upper end of the ranges of variation exhibited by both locations of LPMH femora and the midshaft of recent modern humans, but distinctly higher than the subtrochanteric region of recent modern humans (Fig. 2A).

Significant group differences also are observed in the midshaft and subtrochanteric I_x/I_y ratios (50%: H = 74.115, df = 6, $p < 0.001$; 80%: H = 19.808, df = 6, $p = 0.03$). Specifically, the LPMH group exhibits a midshaft ratio that is consistently above those of other Pleistocene hominins, while the former also tends to exhibit an equally great or greater range of values than other Pleistocene hominin groups at both diaphyseal locations (Fig. 2B). Midshaft I_x/I_y ratios of GM7506 (zero rotation = 1.90, ±5° range = 1.81–1.95) and GM7507 (zero rotation = 1.96, ±5° range = 1.86–2.03) are comparatively high, with only two femora (Zhoukoudian Upper Cave: UC67 = 2.60, UC68 = 2.09) exhibiting higher ratios. In contrast, the midshaft I_x/I_y ratio of GM7508 (zero rotation = 1.24, ±5° range = 1.23–1.24) is much lower, falling towards the lower end of the LPMH range, but still at or above the upper ends of ranges of variation exhibited in other groups (Fig. 2B). At the subtrochanteric region, there is comparatively less separation among groups. The value of GM7508 (zero rotation = 0.66, ±5° range = 0.59–0.75) at this diaphyseal location indicates a mediolaterally elongated cross section that is almost in the middle of the ranges of all groups (i.e., combined Pleistocene hominin and modern human variation).

For midshaft I_{max}/I_{min} (Fig. 2C), values of GM7506 (1.96) and GM7507 (2.06) fall within the upper end of LPMH ranges and above ranges exhibited by all other groups, with only Skhul 5 (right = 1.99, left = 2.22) and Zhoukoudian Upper Cave femora (UC67 = 2.64, UC68 = 2.09) exhibiting higher ratios among the Pleistocene samples. The midshaft ratio of GM7508 (1.24) is substantially lower than those of GM7506 and GM7507, falling towards the lower end of the LPMH range. Thus, midshaft shapes of GM7506 and GM7507 femora are comparatively anteroposterior elongated, both with a pronounced linea aspera and prominent pilaster, while the GM7508 midshaft shape is relatively rounder (Figs. 1 and 2C). At the subtrochanteric region, GM7508 (2.25) falls above Neandertal, LMP, and MH ranges of variation, and within the upper end of LPMH variation.

Pilastric indices of GM7506 (133.5) and GM7507 (134.9)—measured as 126.1 and 127.8, respectively, in Cao et al. (2015)—are larger than those of most Middle/Upper Paleolithic humans, but still within the range of variation of MPMH (i.e., within 1 SD of the mean, u = 124.0 ± 15.6 [$n = 12$]; Trinkaus, 2015). By comparison, the pilastric index of GM7508 (i.e., measured as 111.4 in the present study; measured as 91.4 in Cao et al., 2015) is markedly lower than those of the other Maomaodong partial femora, and closer to the mean of Upper Paleolithic humans and higher than the mean of archaic hominins (i.e., within 2 SD above EP/MP/Nea means; EP: 96.7 ± 13.0 [$n = 6$], MP: 96.5 ± 12.1 [$n = 19$], Neandertals: 99.8 ± 7.6 [$n = 22$]; Trinkaus, 2015) and modern humans (i.e., modern Chinese sample in the present study: 101.1 ± 8.2 [$n = 24$]). Thus, the externally-derived shape ratios are consistent with the CSG-derived shape ratios, where GM7506 and GM7507 are comparatively anteroposteriorly elongated and GM7508 is comparatively rounder.

4. Discussion and conclusions

The Maomaodong femora (GM7506, 7507, 7508) were found to be qualitatively most similar to those of LPMH in terms of surface morphology, notably in their prominent linea aspera and well-developed pilaster (Trinkaus, 2005, 2006), and also quantitatively

in terms of their internal and external shape ratios indicating mediolaterally narrowed midshaft regions. Notably, there is also intragroup variability expressed within the three Maomaodong femora. The linea aspera of GM7508 has a relatively less developed pilaster than those of GM7506 and GM7507, resulting in its comparatively rounder cross-sectional shape at midshaft.

In the femoral midshaft, as has been extensively documented (e.g., Trinkaus and Ruff, 2012; Trinkaus et al., 2014), most Late Pleistocene modern humans have diaphyses in which their anteroposterior dimensions are disproportionately greater than mediolateral dimensions, unlike those of Neandertals (and other archaic humans) that are more proportionate. The degree of expression of the femoral pilaster contributes to this trend. The developed pilasters of GM7506 and GM7507 are reflected in their relatively high pilastric indices and also their relatively high midshaft I_x/I_y and I_{max}/I_{min} ratios. Even though the pilastric index of GM7508 is comparatively lower than those of the other Maomaodong femora, it still falls comfortably within an Upper Paleolithic range of variation (i.e., 89.1–139.0: Trinkaus and Ruff, 2012; Trinkaus, 2015), and is still larger than those of most Holocene modern humans and other Pleistocene hominins prior to the Late Pleistocene. The GM7508 partial femur also exhibits a more mediolaterally elongated subtrochanteric cross section than those of late archaic humans (i.e. Neandertals) and Holocene modern humans, which also aligns it with LPMH features.

Overall features of the Maomaodong four partial mandibles vary little, but rather all are similar in features to those of Late Pleistocene *Homo sapiens* in East Asia (see SOM S1), such as Tianyuan 1 and Upper cave mandibles (Cao et al., 2015). Considering both the features of femora and mandibles, the humans of Maomaodong most closely resemble typical LPMH individuals in morphology. Such an attribution would support the scenario whereby the Maomaodong femora from at least the end of Pleistocene in East Asia exhibit approximately similar morphologies with those of Eurasian early modern humans. Importantly, the Maomaodong femora also document intragroup variability.

The Maomaodong postcranial specimens expand the range of morphological diversity exhibited by East Asian Late Pleistocene humans, particularly femoral diversity, and thus contribute to developing a more thorough understanding of the extent of intragroup structural variation in this region. Morphological variation within East Asian long bone diaphyses that more precisely reflect differences in activity patterns and levels require additional discoveries and more complete specimens to rigorously explore in the future.

Declaration of competing interest

The authors declare that they have no known competing financial interests or personal relationships that could have appeared to influence the work reported in this paper.

Acknowledgements

This work was supported by the Strategic Priority Research Program of Chinese Academy of Sciences (XDB26000000), the National Natural Science Foundation of China (41802020, 41872030, 41630102, 31771325, 91731303), the China Postdoctoral Science Foundation (2017M611449), the Scientific and Technology Committee of Shanghai Municipality (18490750300) for B&R International Joint Laboratory of Eurasian Anthropology, and the 111 Project (B13016).

Supplementary Online Material

Supplementary Online Material to this article can be found online at https://doi.org/10.1016/j.jhevol.2021.102977.

References

Abràmoff, M.D., Magalhães, P.J., Ram, S.J., 2004. Image Processing with ImageJ. Biophot. Int. 11 (7), 36–42.
Bräuer, G., 1988. Anthropologie. In: Knussman, R. (Ed.), Anthropologie. Fischer Verlag, Stuttgart, pp. 160–232.
Cao, B., He, L., Zhang, P., 2015. A study of human fossils discovered at the Maomao Cave site, Xingyi County, Guizhou Province. Acta Anthropol. Sin. 34, 451–460 (in Chinese).
Carlson, K.J., 2005. Investigating the form-function interface in African apes: Relationships between principal moments of area and positional behaviors in femoral and humeral diaphyses. Am. J. Phys. Anthropol. 127, 312–334.
Chen, T., 1989. Accelerator radiocarbon dating for Upper Cave of Zhoukoudian. Acta Anthropol. Sin. 8, 216–221 (in Chinese).
Chen, T., 1992. The second batch of accelerator radiocarbon dates for Upper Cave site of Zhoukoudian. Acta Anthropol. Sin. 11, 112–116 (in Chinese).
Chevalier, T., Özçelik, K., De Lumley, M.-A., Kösem, B., De Lumley, H., Yalçinkaya, I., Taşkiran, H., 2015. The endostructural pattern of a middle pleistocene human femoral diaphysis from the Karain E site (Southern Anatolia, Turkey). Am. J. Phys. Anthropol. 157, 648–658.
Curnoe, D., Ji, X., Liu, W., Bao, Z., Taçon, P.S.C., Ren, L., 2015. A hominin femur with archaic affinities from the Late Pleistocene of Southwest China. PLoS One 10, e0143332.
Han, W., 2005. Analyses of the racial and systematic types of residents of Beiwi Period in Datong, Shanxi Province. Research of China's Frontier Archaeology 4, 270–280 (in Chinese).
IBM Corp., 2017. IBM SPSS Statistics for Windows v. 20.0. IBM Corp., Armonk.
Li, F., Bae, C.J., Ramsey, C.B., Chen, F., Gao, X., 2018. Re-dating Zhoukoudian Upper Cave, northern China and its regional significance. J. Hum. Evol. 121, 170–177.
Puymerail, L., Ruff, C.B., Bondioli, L., Widianto, H., Trinkaus, E., Macchiarelli, R., 2012. Structural analysis of the Kresna 11 Homo erectus femoral shaft (Sangiran, Java). J. Hum. Evol. 63, 741–749.
Rodríguez, L., Carretero, J.M., García-González, R., Arsuaga, J.L., 2018. Cross-sectional properties of the lower limb long bones in the Middle Pleistocene Sima de los Huesos sample (Sierra de Atapuerca, Spain). J. Hum. Evol. 117, 1–12.
Ruff, C.B., 2002. Long bone articular and diaphyseal structure in old world monkeys and apes. I: Locomotor effects. Am. J. Phys. Anthropol. 119, 305–342.
Ruff, C.B., Puymerail, L., Macchiarelli, R., Sipla, J., Ciochon, R.L., 2015. Structure and composition of the Trinil femora : Functional and taxonomic implications. J. Hum. Evol. 80, 147–158.
Shang, H., Trinkaus, E., 2010. The early modern human from Tianyuan Cave, China. Texas A&M University Press, College Station.
Trinkaus, E., 2005. Early Modern Humans. Annu. Rev. Anthropol. 34, 207–230.
Trinkaus, E., 2006. Modern human versus Neandertal evolutionary distinctiveness. Curr. Anthropol. 47, 597–620.
Trinkaus, E., 2015. The appendicular skeletal remains of Oberkassel 1 and 2. In: Giemsch, L., Schmitz, R.W. (Eds.), The Last Glacial Burial from Oberkassel Revisited. Verlag Phillip von Zabern, Darmstadt, pp. 75–132.
Trinkaus, E., Buzhilova, A.P., Mednikova, M.B., Dobrovolskaya, M.V., 2014. The people of Sunghir: Burials, bodies and behavior in the earlier Upper Paleolithic. Oxford University Press, New York.
Trinkaus, E., Ruff, C.B., 1989. Diaphyseal cross-sectional morphology and biomechanics of the Fond-de-Forêt 1 femur and the Spy 2 femur and tibia. Bull. Soc. R. Belge Anthropol. Prehist. 100, 33–42.
Trinkaus, E., Ruff, C.B., 2012. Femoral and tibial diaphyseal cross-Sectional geometry in Pleistocene *Homo*. PaleoAnthropology 13–62.
Villotte, S., Thibeault, A., Sparacello, V., Trinkaus, E., 2020. Disentangling Cro-Magnon: The adult upper limb skeleton. J. Archaeol. Sci. Rep. 33, 102475.
Wei, P., Wallace, I.J., Jashashvili, T., Musiba, C.M., Liu, W., 2017. Structural analysis of the femoral diaphyses of an early modern human from Tianyuan Cave, China. Quat. Int. 434, 48–56.
Wei, P., Lu, H., Carlson, K.J., Zhang, H., Hui, J., Zhu, M., He, K., Jashashvili, T.J., Zhang, X., Yuan, H., Xing, S., 2020. The upper limb skeleton and behavioral lateralization of modern humans from Zhaoguo Cave, southwestern China. Am. J. Phys. Anthropol. 173, 671–696.
Wu, X., 1961. Study on the Upper Cave man of Choukoutien. Vertebr. Palasiat. 6, 181–203 (in Chinese).
Xing, S., Carlson, K.J., Wei, P., He, J., Liu, W., 2018. Morphology and structure of *Homo erectus* humeri from Zhoukoudian, Locality 1. PeerJ 6, e4279.